Journal of Materials Chemistry A

Water Desalination Concept using an Ionic Rectifier based on a Polymer of Intrinsic Microporosity (PIM)

Journal:	*Journal of Materials Chemistry A*
Manuscript ID:	TA-COM-06-2015-004092.R1
Article Type:	Communication
Date Submitted by the Author:	05-Jul-2015

Complete List of Authors:	Madrid, Elena; University of Bath, Chemistry Cottis, Philip; University of Bath, Department of Chemistry Rong, Yuanyang; University of Bath, Chemistry Rogers, Adrian; University of Bath, Physics Stone, James; University of Bath, Physics Malpass-Evans, Richard; Edinburgh University, Chemistry Carta, Mariolino; University of Edinburgh, School of Chemistry McKeown, Neil B; Edinburgh University, School of Chemistry Marken, Frank; Bath University, Department of Chemistry

Journal Name

COMMUNICATION

Water Desalination Concept Using an Ionic Rectifier Based on a Polymer of Intrinsic Microporosity (PIM)

Received 00th January 20xx,
Accepted 00th January 20xx

DOI: 10.1039/x0xx00000x

www.rsc.org/

Elena Madrid [a], Philip Cottis [a], Yuanyang Rong [a], Adrian T. Rogers [b], James M. Stone [c], Richard Malpass-Evans [d], Mariolino Carta [d], Neil B. McKeown [d], and Frank Marken*[a]

We describe ion current rectification using a Polymer of Intrinsic Microporosity (PIM) based on Tröger's base (PIM-EA-TB). When deposited asymmetrically over one (or more) 20 µm diameter hole(s) in 6 µm thick poly(ethylene terephthalate) and investigated in a two-compartment electrochemical cell with acidified aqueous NaCl on both sides, novel ionic diode effects are observed.

Ionic diode phenomena (i.e. rectification effects in ion flow across polarised membranes) are observed in biological membrane pores,[1] in nano-fluidic devices,[2] and at gel interfaces.[3] They are of considerable interest in analytical detection methods[4] and also have potential in energy harvesting.[5] Our recent work has demonstrated that a *materials chemistry approach* (in contrast to the *nanofabrication approach*) to ionic diodes is possible[6] based on employing novel polymers of intrinsic microporosity (PIMs). Previously, we demonstrated the anion absorption capacity of an amine-containing PIM derived from Tröger's base (PIM-EA-TB; Fig. 1)[7] and the opportunities arising from embedding water-insoluble molecular catalysts[8] or gold nano-catalysts[9] into the rigid PIM host framework. Whilst investigating the ion transport through a PIM-EA-TB film, we discovered that *pH* gradients across the membrane cause rectification of ion flow or an "ionic diode" effect.[6] In this study, this ion flow rectification effect is investigated in more detail, and new opportunities are proposed arising from being able to operate the ionic diode using sea water and without an externally imposed a *pH* gradient. Hence, we propose that this approach provides a novel concept for low energy water desalination.

PIM-EA-TB (Fig. 1; M_w = 70 kD, BET surface area = 1027 m^2g^{-1}) is a highly rigid polymer that has two interacting amine sites per repeat unit that was developed originally for use as a material for gas separation membranes[10] and is prepared via a polymerisation reaction based on Tröger's base formation.[11] PIM-EA-TB is a member of a wider class of PIM materials, which are solution processable polymers which behave as microporous materials due to their high rigid and contorted macromolecular shapes and inability to pack space efficiently.[12]

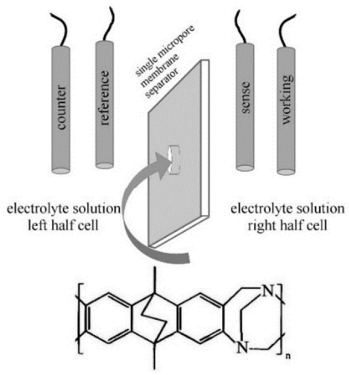

Figure 1. Experimental configuration of the ionic diode and the molecular structure of PIM-EA-TB.

PIM-EA-TB is readily dissolved into chloroform solution‡ and then deposited by solvent evaporation into a 20 µm diameter pore in a PET film, (Figure 1). In order to achieve "asymmetric" deposits (*vide infra*) the PET film is initially placed onto a film of 1% agarose gel, the PIM-EA-TB solution is applied, and after evaporation the PET film is removed from the agarose gel. Electrochemical phenomena are studied with four-electrode polarisation of the membrane exposed to aqueous NaCl.

Due to its intrinsic microposity, PIM-EA-TB is able to conduct both cations and anions.[6] When in the protonated state, the flow of ions across the membrane is restricted and dominated by anions. Under conditions of asymmetric *pH* in left and right half cells, an interfacial "depletion layer"[6] develops, for example, when placed between 10 mM NaOH and 10 mM HCl in the left and right hand side of the membrane cell, respectively. Figure 2 shows typical voltammograms

[a] Dr. Elena Madrid, Philip Cottis, Yuanyang Rong, Prof. Frank Marken, Department of Chemistry, University of Bath, Bath BA2 7AY, UK, Email F.Marken@bath.ac.uk
[b] Dr. Adrian T. Rogers, Microscopy and Analysis Suite, Department of Physics, University of Bath, Bath BA2 7AY, UK
[c] Dr. James M. Stone, Centre for Photonics and Photonic Materials, Department of Physics, University of Bath, Bath BA2 7AY, UK
[d] Dr. Richard Malpass-Evans, Dr. Mariolino Carta, Prof. Neil B. McKeown, School of Chemistry, University of Edinburgh, Joseph Black Building, David Brewster Road, Edinburgh, Scotland EH9 3FJ, UK

† Footnotes relating to the title and/or authors should appear here.
Electronic Supplementary Information (ESI) available: [details of any supplementary information available should be included here]. See DOI: 10.1039/x0xx00000x

for a 20 µm pore in PET filled with PIM-EA-TB for both configurations. A strong ionic diode effect is observed with a rectification constant of ca. 100 (measured at +/- 2V). When switching the two solutions between left and right, the diode effect is reversed (see red and blue trace in Figure 2). This behaviour was attributed previously to the annihilation of hydroxide (driven into the membrane by negative applied potential) and protons (see scheme in Figure 2).

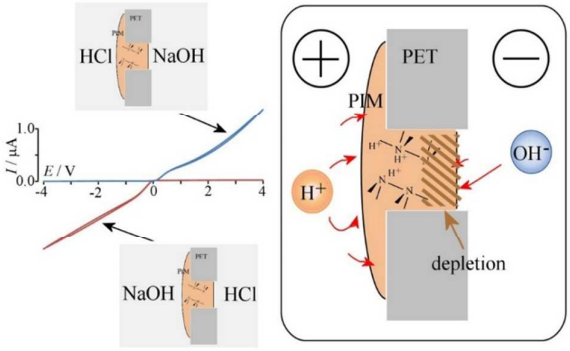

Figure 2. Voltammograms (scan rate 0.01 V s^{-1}) for a PIM-EA-TB membrane between 10 mM HCl and 10 mM NaOH. The schematic drawing describes the depletion layer formation.

When investigating the symmetric case with the same solution on both sides (aqueous NaCl; *pH* = 2), a "secondary" ionic diode effect is observed, but only at asymmetrically deposited PIM-EA-TB films. Figure 3A shows voltammograms for *pH* = 2 aqueous solutions and for different NaCl concentrations. The asymmetry in the current response or "ionic diode effect" for this case is caused by the asymmetry in the geometry of the PIM-EA-TB deposit. The narrow pore causes a 20 µm diameter disk-shaped PIM-polymer|aqueous electrolyte interface on one side and a much larger PIM-polymer|aqueous electrolyte interface on the opposite side (see fluorescence microscopy images in Figure 4). With applied potential the small interface can be polarised with loss of highly mobile protons, which causes a depletion effect with resulting current rectification (Figure 3).

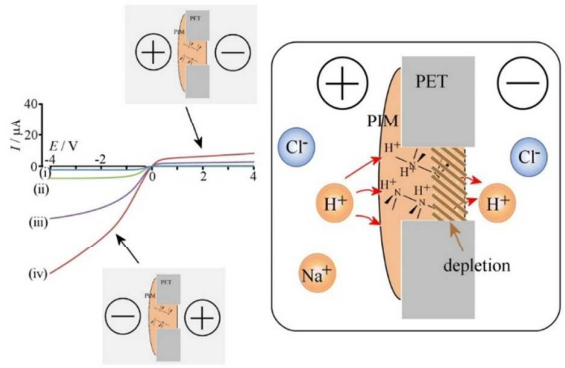

Figure 3. Voltammograms (scan rate 0.02 Vs^{-1}) for a symmetric electrolyte cell with (i) 0.05, (ii) 0.1, (iii) 0.5, and (iv) 1.0 mol dm^{-3} NaCl acidified to pH 2. A schematic drawing is shown to explain the effect of the asymmetric membrane deposit.

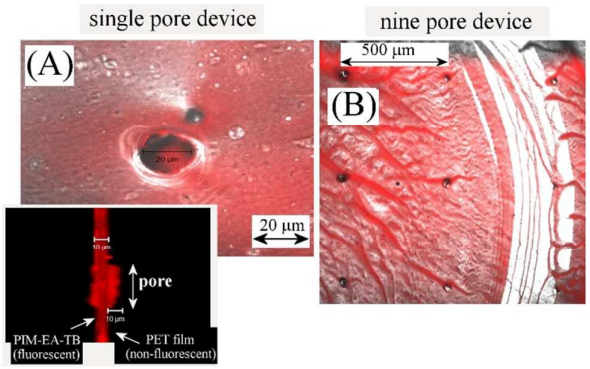

Figure 4. Fluorescence microscopy images showing the PIM-EA-TB on PET after immersion into ethanolic eosin Y. The PET film is not visible but the PIM-EA-TB deposit is stained. (A) A single pore with asymmetric PIM-EA-TB filling (inset) and (B) a nine pore film are shown.

The origin of this ion-flux dependent ionic diode effect can be further investigated by systematically changing the *pH* of the solution. Figure 5A shows a set of voltammograms obtained at *pH* = 2, 3, 4, 5, 6, and 12. A well-defined rectification effects is observed at *pH* = 2 and 3. When increasing the *pH* to 4 or 5 the effect is reduced and with further increase in alkalinity the ion current through the PIM-EA-TB membrane finally appears symmetric without rectification.

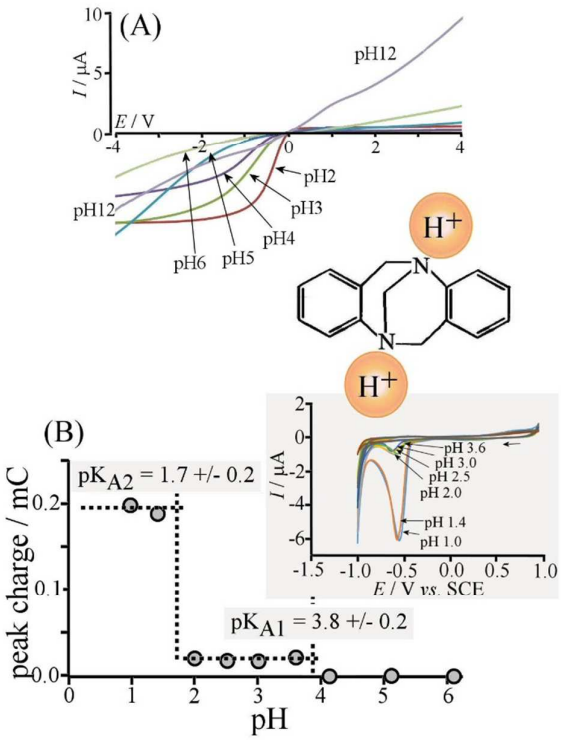

Figure 5. (A) Voltammograms (scan rate 0.02 Vs^{-1}) for a symmetric electrolyte cell with 0.1 mol dm^{-3} NaCl acidified to *pH* = 2, 3, 4, 5, 6, and 12. (B) Plot of proton reduction charge versus *pH* with experimental pK_A values. The inset shows cyclic voltammograms (scan rate 0.02 Vs^{-1}) for 3 µg PIM-EA-TB on a 1 mm diameter Pt disc "loaded" with protons in buffer and then transferred into 0.1 M $NaClO_4$ for proton reduction.

This transition in diode behaviour with *pH* can be traced to the protonation of the tertiary nitrogen sites in the Tröger's base units of PIM-EA-TB (Figure 5). Based on predictive (ACDlabs) estimation of the pK_{A1}, the first protonation step should occur at around *pH* = 4 consistent with the onset of the ionic diode effect. Measurements of proton uptake into the PIM-EA-TB film with *pH* (Figure 5B) confirm that pK_{A1} = 3.8 +/- 0.2 and pK_{A2} = 1.7 +/- 0.2 (note the increase in charge for the second protonation presumably due to some loss of structural rigidity). This further confirms the suggested mechanism for the formation of the depletion layer based on proton loss. Additional experiments with 1-pore, 3-pore, and with 9-pore PET films (see Figure 4) resulted in rectification ratios of 6, 7, and 3 (at +/-2 V), respectively, consistent with some decrease in ionic diode efficiency when the number of pores is increased. In future the multi-pore rectification ratio needs to be improved and with appropriate structural tuning of PIM-EA-TB, the pK_{A1} value can be shifted into the neutral *pH* range to allow rectification in less acidic media such as seawater.

The symmetry effects observed for the ion flow through the PIM-EA-TB membrane is striking and perhaps unexpected. With the mechanism based on an interfacial deprotonation effect, it is interesting to explore chronoamperometry experiments in addition to the voltammetry study. Figure 6A shows the steady state current trace for a PIM-EA-TB membrane placed between two half cells with 0.5 M NaCl at *pH* = 2. A rectification effect is evident (this is less strong when compared to that in Figure 4A due to the higher ionic strength) with the potentials for chronoamperometry selected at +1 V and -1V. Figure 6B and 6C show chronoamperometry data with a transient feature observed for both "opening" the diode at -1 V and "closing" the diode at +1V. The transient charge for diode "opening" (see Figure 6C) amounts to approximately 10 μC. The charge equivalent to single protonation of the PIM-EA-TB within the PET pore (6 μm thick, 20 μm diameter) is approximately 0.3 μC, which suggests that the diode "opening" process is dominated by additional cross-current flow. The transient charge for diode "closing" is an order of magnitude smaller and likely to be associated mainly directly with the PIM-EA-TB deprotonation within the pore leading to the rectification effect.

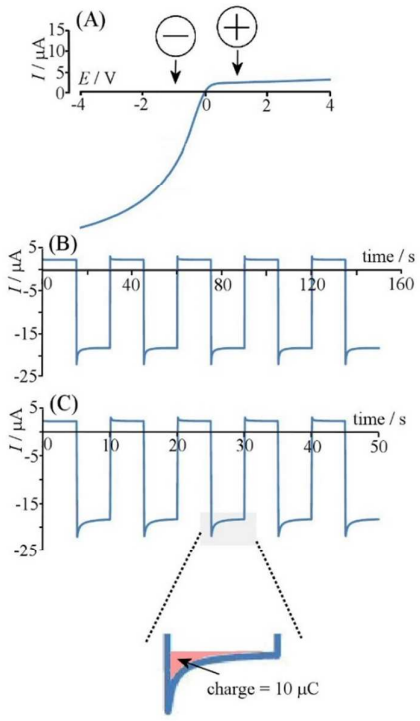

Figure 6. (A) Voltammogram (scan rate 0.02 Vs^{-1}) for a PIM-EA-TB membrane in 0.5 M NaCl pH 2. (B,C) Chronoamperometry data for the membrane when switched between +1 V and -1V.

The future application of the ionic diode effect for a low energy seawater desalination process appears appealing. Currently, the main desalination technology[13] is energy intensive and based on a high pressure reverse osmosis[14] with severe problems such as membrane blocking. Capacitive desalination[15] offers a novel lower energy batch method. Recently, also new microfluidic methods have been proposed, but these are probably associated with flaws in scale up due to resistivity in microchannels and due to lower energy efficiency due to DC polarisation/electrolysis.[16] Here, the ionic diode is considered like an "ionic circuit element" that can be combined with a "cationic resistor" (usually a semi-permeable Nafion™ membranes[17]). The rectification effect due to the PIM-EA-TB membrane asymmetry can be exploited in a process similar to AC to DC rectification in electronic components. Operation in AC mode could provide further benefits in avoiding batch operation and lowering total resistance. A schematic ionic circuit description of the system based on controlled ion flux is given in Figure 7.

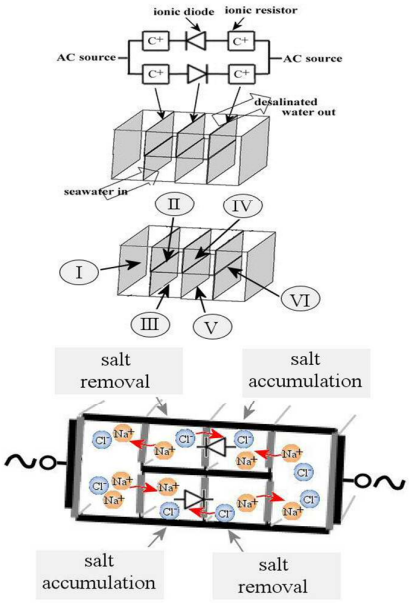

Figure 7. Schematic drawing of a desalination system based on 6 flow chambers where AC stimulation is causing salt depletion in chambers II and V at the same time as salt accumulation in chambers IV and III. Due to the AC stimulation detrimental electrolysis can be avoided with operation at low energy demand.

The system is based on six chambers with PIM-EA-TB membrane centrally separating chambers II and IV and III and V with opposite rectification direction. A potential applied across this system will "open" one anion channel and "close" the second one. An additional cation exchange membrane (Nafion™) is connecting chambers I and II, I and III, VI and IV, and VI and V. With chloride anions allowed in one direction, only a corresponding sodium cation flux with complement the ion flux leading to build up of salt in one cell and loss of salt in the other. Polarisation of the outer electrodes left and right will gradually start unwanted electrolysis reactions and therefore the polarisation has to be reversed (AC stimulation is applied) to avoid electrolysis. This will open the second diode and lead to the same net salt transfer in the bottom two chambers. The overall efficiency of this desalination system will be depending on (i) how effective the PIM-EA-TB membrane can switch, (ii) the rectification ratio at a given *pH*, (iii) the amplitude of polarisation and the design/impedance of the outer electrodes.

Conclusions

A novel materials chemistry approach can be employed for the development of ionic rectifiers. It has been shown that asymmetric membrane geometry is sufficient to allow ionic diode effects and rectification in PIM-EA-TB to occur with potential future applications in desalination. Aqueous NaCl solutions from low to high salinity were investigated and the *pH* (or pK_A) was shown to be crucial in optimising the rectification ratio (= desalination efficiency). The best ionic diode effects were observed at pH 2 and 3 due to the intrinsic PIM-EA-TB protonation (pK_{A1}) and therefore using PIMs with different pK_{A1} values will allow further adjustments to be made. Ultimately, we anticipate that the shift of pK_{A1} by approximately 3 pH units into the neutral will allow efficient desalination even in natural sea water. However, many parameters including membrane thickness and pore number and diameter will have to be studied and optimised as well. The proposed desalination concept based on an AC circuit (operating analogously to an electronic rectifier) will have the significant advantage that no direct electrolysis would be required (i.e. only non-Faradaic charging currents at the driver electrodes). In contrast to existing desalination technology, this methodology is predicted to provide benefits in low cost and low energy consumption especially for partial desalination.

Acknowledgement. E.M. and F.M. acknowledge financial support from the EPSRC (EP/K004956/1).

Notes and references

‡ *Chemical Reagents.* Sodium chloride, sodium hydroxide (≥98%), ethanol, and eosin Y were purchased from Sigma-Aldrich and concentrated hydrochloric acid (32%) from Fisher Scientific. Ultra-pure water, with a resistivity of not less than 18.2 MΩ cm, was supplied by an ELGA Purelab Classic system and used for preparation of all the electrolyte solutions.

Instrumentation and Procedures. Transport properties of a single PET pore were studied by voltammetry using an Eco Chemie Autolab PGSTAT12 potentiostat controlled with GPES 4.7 software. Cyclic voltammograms were recorded from a potential window of -4 V ≤ E ≤ 4 V. A scan rate of 20 mV s^{-1} was used for all the measurements. Two glass half-cells with flange to secure the PET membrane were used. Silicone film seals were employed between glass and PET film and a metal clamp permitted to hold the cells in place. The compartments of the two half-cells were filled equally with the sodium chloride solution. Ion currents were measured using a four electrode system. A transmembrane potential was applied through the working and counter electrodes (Pt wires). The sensor and reference electrodes (KCl-saturated calomel electrodes, SCE) defined the potential across the single pore.[6]

In order to prepare the PET pore, a laser drilling technique was used to produce a 20 µm diameter single pore on a poly(ethylene terephthalate) (PET) film of 6 µm thickness. Initially, films of 25 cm^2 were cut for better manipulation. The laser used (Fianium Ltd.) emits pulses of 5 ps duration at a wavelength of 1064 nm with a repetition rate of 20 MHz. The pulses had a normal frequency chirp and were then compressed to 320 fs by a grating compressor pair and frequency doubled by a lithium triborate crystal (LBO) to 532nm. The light was then launched into a hollow core negative curvature fibre with a core diameter of 16 µm and a low numerical aperture (0.04). The other end of the fibre was brought to within a few tens of microns of the PET film. An exposure of the film to the laser of at least 30 s ensured a macro hole of 20 µm diameter in the PET film. PET films with three or nine pores were prepared in the same way.

The single PET hole was coated with a PIM-EA-TB (PET film on 1% agarose gel; 10 µL of a solution 1 mg mL^{-1} in chloroform). The solvent was allowed to air dry and the PET then lifted off the agarose gel to give asymmetric deposits. For fluorescence analysis, ethanolic eosin Y was employed to colour the PIM-EA-TB component without affecting the PET film. This was achieved by immersion of the modified PET film in 1 mM eosin Y in ethanol-water solution (50:50) for at least 3h. A laser scanning confocal system (Carl Zeiss LSM510Meta) was employed with an inverted microscopy based on an Axiovert 200M to map PIM-EA-TB within

the film when eosin Y was excited using a HeNe laser at 543 nm 30%. Long Pass (LP) 560nm was used as emission filter. Image stacks 17 µm in total depth were acquired at 1 µm intervals using the EC Plan-Neofluar 20x/0.5 Ph2 objective. The intensity of fluorescence was adjusted using the smart gain to ensure brightest of the dye was maximal without being saturated and the background was corrected using Zeiss LSM v.4.2 software. These adjustments remained constant for imaging experiments.

1 W. Guo, Y. Tian and L. Jiang, *Acc. Chem. Res*., 2013, **46**, 2834.
2 (a) L. Krasemann and B. Tieke, *Langmuir*, 2000, **16**, 287; (b) J.H. Han, K.B. Kim, H.C. Kim and T.D. Chung, *Angew. Chem*., 2009, **48**, 3830; (c) Z. Siwy, A. Fulinski, *Phys. Rev. Lett*., 2002, **89**, 198103; (d) M. Ali, P. Ramirez, S. Mafe, R. Neumann and W. Ensinger, *ACSNano*, 2009, **3**, 603; (e) K. Zielinska, A.R. Gapeeva, O.L. Orelovich and P. Yu. Apel, *Nucl. Instr. Methods Phys. Res. B*, 2014, **326**, 131.
3 (a) M. Eigen and L. Demaeyer, *Zeitschrift Elektrochem*., 1955, **59**, 986; (b) B. Lovrecek, A. Despic and J.O.M. Bockris, *J. Phys. Chem.,* 1959, **63**, 750; (c) L. Hegedus, Z. Noszticzius, A. Papp, A.P. Schubert and M. Wittmann, *ACH-Models Chem.,* 1995, **132**, 207.
4 Y.F. Liu and L. Yobas, *Biosens. Bioelectron.,* 2013, **50**, 78.
5 J. Gao, W. Guo, D. Feng, H.T. Wang, D.Y. Zhao and L. Jiang, *J. Amer. Chem. Soc*., 2014, **136**, 12265.
6 E. Madrid, Y. Rong, M. Carta, N.B. McKeown, R. Malpass-Evans, G.A. Attard, T.J. Clarke, S.H. Taylor, Y.T. Long and F. Marken, *Angew. Chem*., 2014, **53**, 10751.
7 F. Xia, M. Pan, S.C. Mu, R. Malpass-Evans, M. Carta, N.B. McKeown, G.A. Attard, A. Brew, D.J. Morgan and F. Marken, *Electrochim. Acta,* 2014, **128**, 3.
8 Y.Y. Rong, R. Malpass-Evans, M. Carta, N.B. McKeown, G.A. Attard and F. Marken, *Electrohem. Commun*., 2014, **46**, 26.
9 Y.Y. Rong, R. Malpass-Evans, M. Carta, N.B. McKeown, G.A. Attard and F. Marken, *Electroanalysis*, 2014, **26**, 904.
10 M. Carta, R. Malpass-Evans, M. Croad, Y. Rogan, J. C. Jansen, P. Bernardo, F. Bazzarelli and N. B. McKeown, *Science*, 2013, **339**, 303.
11 (a) M. Carta, M. Croad, J. C. Jansen, P. Bernardo, G. Clarizia and N.B. McKeown, *Polymer Chem.,* 2014, **5**, 5255; (b) M. Carta, M. Croad, R. Malpass-Evans, J. C. Jansen, P. Bernardo, G. Clarizia, K. Friess, M. Lanc and N. B. McKeown, *Adv. Mater.,* 2014, **26**, 3526; (c) M. Carta, R. Malpass-Evans, M. Croad, Y. Rogan, M. Lee, I. Rose and N. B. McKeown, *Polymer Chem.,* 2014, **5**, 5267.
12 (a) P. M. Budd, E. S. Elabas, B. S. Ghanem, S. Makhseed, N. B. McKeown, K. J. Msayib, C. E. Tattershall and D. Wang, *Adv. Mater.,* 2004, **16**, 456; (b) P. M. Budd, B.S. Ghanem, S. Makhseed, N.B. McKeown, K.J. Msayib and C.E. Tattershall, *Chem. Commun.,* 2004, 230; (c) N.B. McKeown and P.M. Budd, *Chem. Soc. Rev.,* 2006, **35**, 675; (d) M. Carta, K.J. Msayib, P.M. Budd and N.B. McKeown, *Org. Lett.,*2008, **10**, 2641; (e) D. Fritsch, G. Bengtson, M. Carta and N.B. McKeown, *Macromol. Chem. Phys.,* 2011, **212**, 1137; (f) R. Short, M. Carta, C.G. Bezzu, D. Fritsch, B.M. Kariuki and N.B. McKeown, *Chem. Commun.,* 2011, **47**, 6822; (g) C.G. Bezzu, M. Carta, A. Tonkins, J.C. Jansen, P. Bernardo, F. Bazzarelli and N.B. McKeown, *Adv. Mater.,* 2012, **24**, 5930; (h) Y. Rogan, L. Starannikova, V. Ryzhikh, Y. Yampolskii, P. Bernardo, F. Bazzarelli, J.C. Jansen and N.B. McKeown, *Polymer Chem.,* 2013, **4**, 3813; (i) Y. Rogan, R. Malpass-Evans, M. Carta, M. Lee, J.C. Jansen, P. Bernardo, G. Clarizia, E. Tocci, K. Friess, M. Lanc and N.B. McKeown, *J. Mater. Chem., A,* 2014, **2**, 4874.
13 J. Zhou, V.W.C. Chang and A.G. Fane, *Water Res.*, 2014, **61**, 210.
14 S. Liyanaarachchi, L. Shu, S. Muthukumaran, V. Jegatheesan and K. Baskaran, *Rev. Environm. Sci. Bio-Technol.*, 2014, **13**, 203.
15 F.A. AlMarzooqi, A.A. Al Ghaferi, I. Saadat and N. Hilal, *Desalination*, 2014**, 342**, 3.
16 K.N. Knust, D. Hlushkou, R.K. Anand, U. Tallarek and R.M. Crooks, *Angew. Chem.*, 2013, **52**, 8107.
17 R.S.L. Yee, R.A. Rozendal, K. Zhang and B.P. Ladewig, *Chem. Engineer. Res. Design*, 2012, **90**, 950.

Graphical Abstract

Title: Water Desalination Concept Using an Ionic Rectifier based on a Polymer of Intrinsic Microporosity (PIM)

Authors: Elena Madrid, Philip Cottis, Yuanyang Rong, Adrian T. Rogers, James M. Stone, Richard Malpass-Evans, Mariolino Carta, Neil B. McKeown, and Frank Marken

A polymer with intrinsic microporosity, when immobilized into 20 μm pores, is shown to result in ionic rectification effects due to geometric asymmetry with potential for future applications in desalination.